*J. King Saud Univ.*, Vol. 6, *Eng. Sci.* (2), pp. 149-166 (A.H. 1414/1994)

# Stress-Strain Relationship for Concrete Confined by Rectilinear Reinforcement: A Stiffness Degradation Approach

**Abdulrahman H. Al-Shaikh**

*Civil Engineering Department, College of Engineering, King Saud University, P.O. Box 800, Riyadh 11421, Saudi Arabia*

(Received 16/11/1992; accepted for publication 16/4/1993)

**Abstract.** Square tied concrete prisms were tested under uniaxial concentric compressive load. Test variables were the tie spacing and diameter (3 levels each). Based on the observed degradation of the prism's longitudinal stiffness, a simplified analytical stress-strain relationship was derived. The proposed model takes into account the effect of the tie spacing and diameter on the prism's tangent stiffness, as well as the maximum stress and corresponding strain. Comparison of the analytical and experimental stress-strain diagrams indicated a very good correlation.

## Introduction

The use of transverse reinforcement to confine the concrete compression members has been widely accepted as a practical means of improving the member's strength and ductility. This improvement in the compressive strength and deformability of confined concrete is the result of the resistance offered to the concrete lateral expansion by the confining reinforcement. The reinforcement is thereby tensioned, leading to the reduction in the rate of the concrete lateral expansion with respect to the applied axial stress. The confining stresses therefore depend on the applied axial stress, the concrete stiffness, the stiffness and uniformity of distribution of the confining reinforcement, free span of ties, volumetric ratio , and ratio of the core area to the gross area.

Steel spirals and stirrups (or ties) are the two most common methods used for providing lateral confinement to concrete columns. Both methods were the focus of

many investigations in the past [1-10], where the effect of various parameters on the confined concrete behavior was reported. These parameters include the confining steel diameter, spacing, volumetric ratio and initial stress as well as other factors such as concrete strength, presence of concrete cover, loading rate and strain gradient. An increase in strength and enhancement in ductility was reported with the increase of the confinement steel diameter (d) and the decrease in its spacing (s). In addition, a number of analytical expressions for the stress-strain relationship, the maximum stress ($\sigma_m$) and the corresponding maximum strain ($\varepsilon_m$) were also developed by the various investigators. These expressions, however, vary greatly in form and in the extent to which the various parameters are accounted for. A comprehensive review of previous work on confined concrete columns is presented in reference [11].

The experimental results of compressive tests performed on concrete prisms with tie confinement were investigated in this paper. The main test variables were the ties diameter and spacing. A stiffness degradation approach for describing their stress-strain behavior, similar to the one used by Cheong [12], was adopted. In this approach, the prisms longitudinal tangent stiffness ($E_t$) was observed and its reduction with the increase in the prism longitudinal strain was idealized by a bi-linear relationship. The slope of the two linear portions were then used in conjunction with the ties diameter and spacing to develop a stress-strain relationship which compared very accurately with the experimental results.

## Specimen and Material Details

The overall dimensions of the tested prisms were 150 mm × 150 mm × 450 mm. A prism height to width ratio of 3 was chosen so that the influence of end restraints, caused by frictional forces that develop at the prism-loading platen interfaces on the behavior of the mid-height section would be negligible. Lateral confinement was provided by square mild steel ties with three different diameters of 4,6 and 8 mm; and were also spaced at three different distances of 30,45 and 60 mm. Full specimen details are presented in Table 1 and Fig. 1. Typical tie stress-strain curve is also presented in Fig. 2. Four longitudinal bars ($\phi$ 4 mm) were placed at the corners of each prisms for the main purpose of holding the ties in place. This resulted in a very low longitudinal reinforcement ratio and, therefore, their effect on the prisms stiffness can be neglected. A concrete mix with proportions of 1: 2: 2.3 by weight with a maximum aggregate size of 10 mm, free w/c ratio of 0.51 was used. All prisms were cast in the vertical position, cured under water for 7 days tested at the age of 28 days. A minimum of 3 identical prisms for each test variable were tested. In addition, control cylinders were also cast and tested at the same age.

**Table 1. Specimen details**

| Group | No. of specimens | Mean strength (MPa) | Ties | | | | $A_{core}$ / $A_{gross}$ |
|---|---|---|---|---|---|---|---|
| | | | s(mm) | d(mm) | Volumetric ratio % | $f_y$ (MPa) | |
| C1 | 3 | 36 | 30 | | 0.97 | | |
| C2 | 3 | 34 | 45 | 4 | 0.63 | 316 | 0.77 |
| C3 | 4 | 33 | 60 | | 0.49 | | |
| C4 | 3 | 37 | 30 | | 2.19 | | |
| C5 | 3 | 35 | 45 | 6 | 1.41 | 350 | 0.73 |
| C6 | 4 | 34 | 60 | | 1.10 | | |
| C7 | 3 | 43 | 30 | | 3.89 | | |
| C8 | 3 | 39 | 45 | 8 | 2.50 | 380 | 0.68 |
| C9 | 4 | 37 | 60 | | 1.95 | | |

- $f_y$ for longitudinal steel = 316 MPa

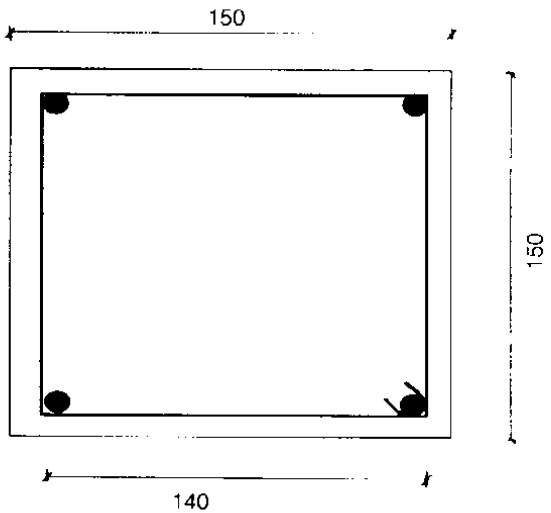


**Fig. 1. Typical specimen cross-section (dimensions in mm).**

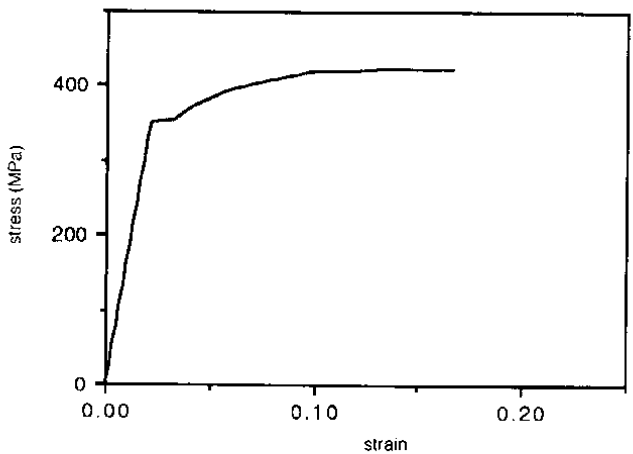


**Fig. 2. Typical tie stress-strain curve (6 mm diam.).**

## Loading and Instrumentation Details

All prisms were tested monotonically in compression in an Amsler universal testing machine. Both, the middle third and overall (between platens) concrete strains were measured using 8 LVDT's (2 at each prism face) with a gauge length of 100 mm. The difference in the strain readings between the four faces ranged from about 2.5 to 11%; therefore, an average reading was taken. Ties strains at the middle third were also measured using 4 electrical resistance strain gauges. The applied load and the measured strains were recorded and analyzed using an HP mini computer and data acquisition system.

## Analysis of the Results

A typical stress-strain curve of the tested prisms is shown in Fig. 3. Only middle third strains were used in producing this and the subsequent figures. A close observation of the prisms longitudinal stress-strain behavior indicated, basically, a two-stages of response up to the maximum load. In the first stage, the concrete was relatively intact recording a smaller longitudinal strains, and consequently, smaller confining stress with the increase in applied load. The seond stage was marked by a much higher longitudinal strain than in the first stage without a stress increase of a similar

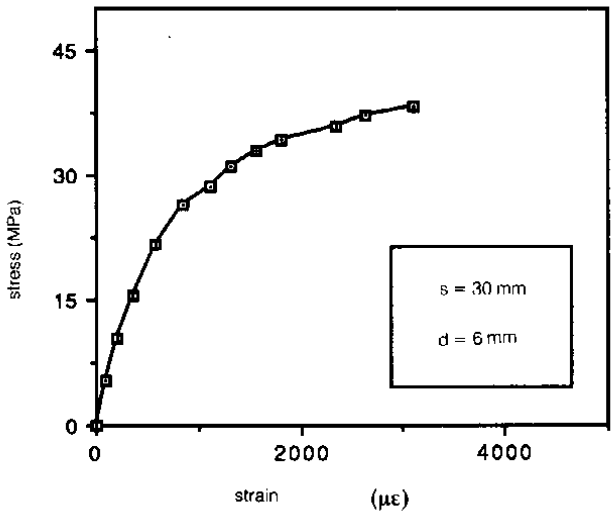


**Fig. 3. Typical stress-strain curve of a tested prism.**

magnitude. This, in turn, led to a continuous decrease in the longitudinal stiffness until the end of this stage, at maximum load. These observations suggested a further investigation into the manner in which the prism stiffness degraded with stress and strain. In order to do this, graphs of the following relations for all tested prisms were obtained:

a) $E_{sec}$ -σ
b) $E_{sec}$ -ε
c) $E_t$ -σ
d) $E_t$ -ε

where ($E_{sec}$) is the secant stiffness and ($E_t$) is the tangent stiffness at any point (σ,ε) on the stress-strain curve. Values of $E_t$ were evaluated at any point ($\sigma_v$ , $\varepsilon_v$) using Taylor's expansion. After neglecting derivatives of order higher than two, the equation for $E_t$ is given as:

$$E_t = \frac{(\varepsilon_v - \varepsilon_u)^2 \sigma_w - [(\varepsilon_v - \varepsilon_u)^2 - (\varepsilon_w - \varepsilon_v)^2]\ \sigma_v - (\varepsilon_w - \varepsilon_v)^2 \sigma_u}{(\varepsilon_v - \varepsilon_u)(\varepsilon_w - \varepsilon_v)(\varepsilon_w - \varepsilon_u)} \qquad (1)$$

The point ($\sigma_u$ , $\varepsilon_u$) are close to, and slightly smaller than the point ($\sigma_v$ , $\varepsilon_v$), while the point ($\sigma_w$ , $\varepsilon_w$) are close to, and slightly larger than the point ($\sigma_v$ , $\varepsilon_v$).

All plotted relations indicated continuous deterioration of stiffness up to ($\sigma_m$ , $\varepsilon_m$). Typical plots from different test groups are shown in Figs. 4 to 7. Similar behavior for all tested specimens were also obtained. Comparison of the various plots indicated that stiffness degradation with stress did not follow a readily quantifiable trend that can be used for describing the prism behavior. The degradation of stiffness with strain, on the other hand, showed a more consistent and quantifiable trends for all prisms. The ($E_{sec}$) curves showed a regular and smooth reduction in stiffness while the ($E_t$) curves reflected the two-stage behavior mentioned earlier as can be seen in Fig. 7. As can be seen from these figures, the ($E_t - \varepsilon$) curves consisted mainly of two approximately linear portions. The first line corresponds to the portion of loading where most of the stiffness degradation occured, over a relatively small longitudinal strain. The second line has a much lower gradient and corresponds to the loading part where most of the longitudinal strain occured, and where the longitudinal stiffness gradually reduced to zero. The slopes of the two lines ($S_1$) and ($S_2$)

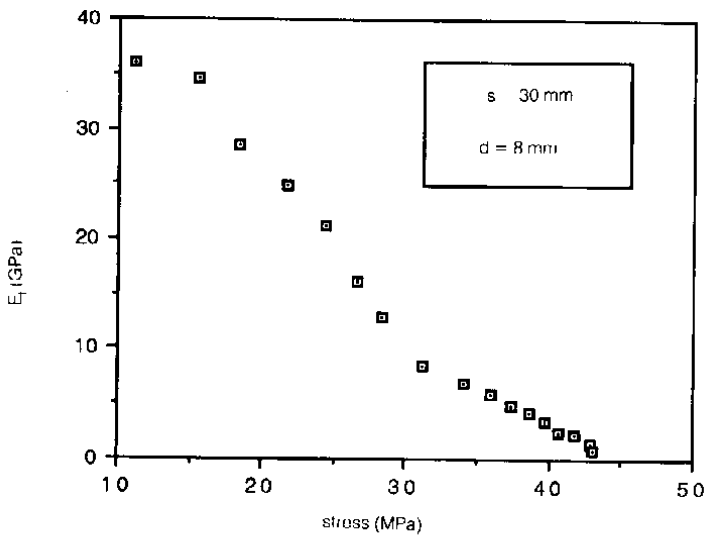


**Fig. 4. Variation of $E_t$ with axial stress.**

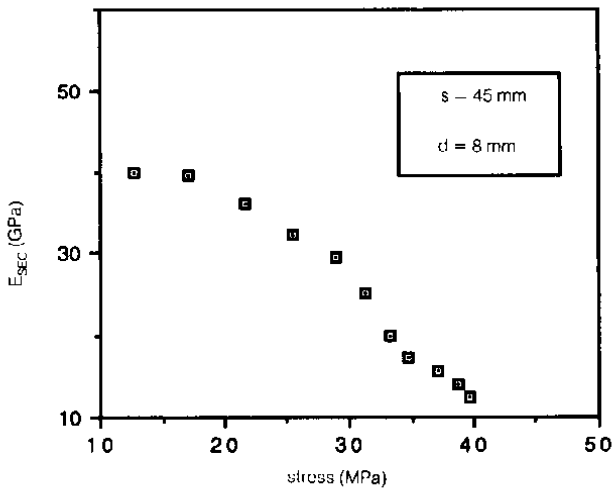


**Fig. 5. Variation of $E_{SEC}$ with axial stress.**

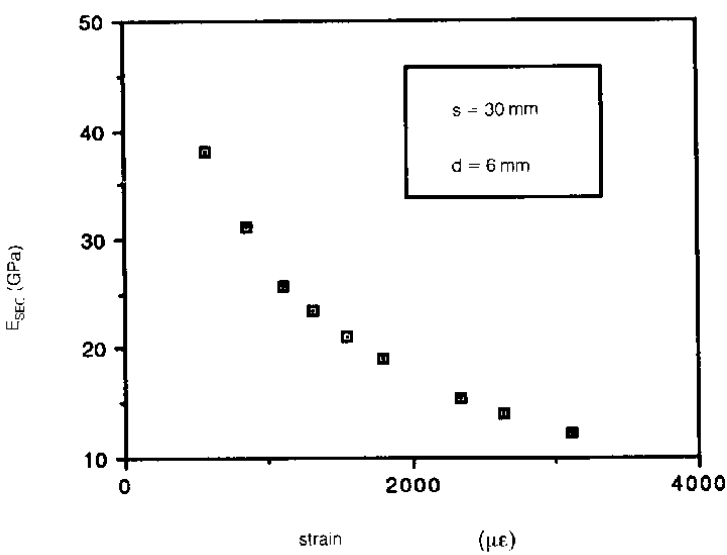


**Fig. 6. Variation of $E_{SEC}$ with axial strain.**

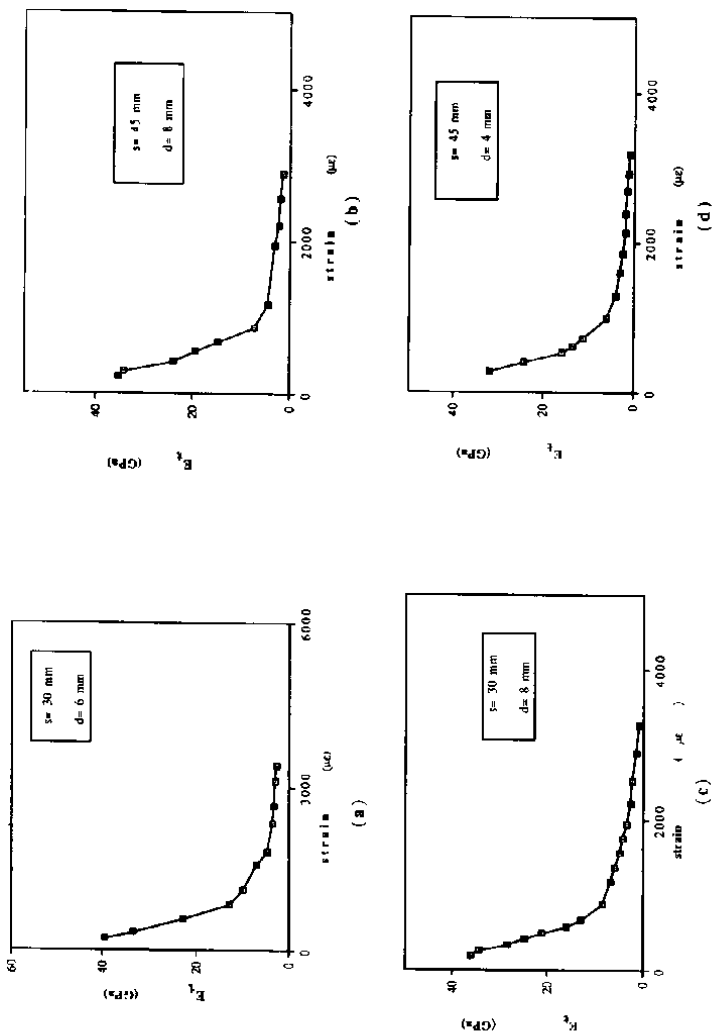


Fig. 7. Variation of $E_t$ with axial strain.

were obtained by two separate linear regression analysis of the ($E_t$ – ε) relation of every prism. The two regression lines for prism P1 (group C3) are shown in Fig. 8.

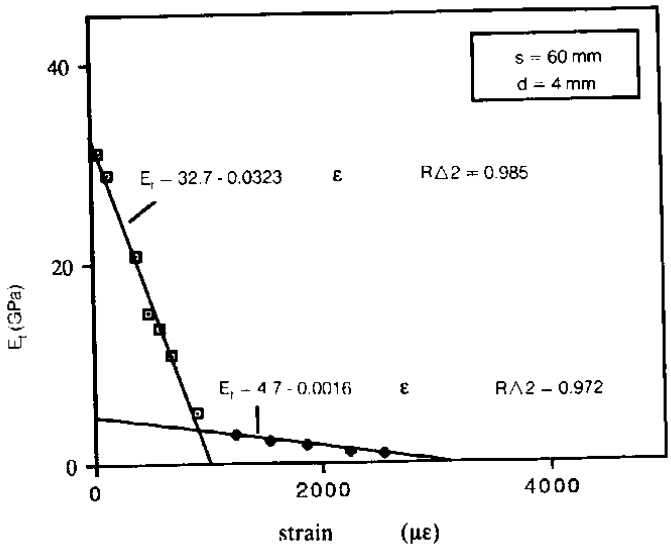


**Fig. 8. Regression lines of $E_t$ ε relationship for prism P1.**

The obtained values of the two slopes ($S_1$ and ($S_2$), as well as ($\sigma_m$) and ($\varepsilon_m$) for all prisms were then plotted against the two test variables, the ties diameter (d) and spacing (s). The variation of $S_2$ with the tie spacing is shown in Fig. 9, while Fig. 10 is showing the variation of $\sigma_m$ with the tie diameter. When the effect of one test parameter was investigated in these figures, the other parameter was held constant. The volumetric ratio was, however, changing. It should be noted that each point on these figures represent an average of three values. A simple linear fit to the data was then performed from which the following relationships for the slope $S_1$ were obtained:

$$S_1 = -66.58 + 0.8\,s \qquad (MPa/\mu\varepsilon) \qquad (2a)$$

$$S_1 = -19.56 + 1.67\,d \qquad (MPa/\mu\varepsilon) \qquad (2b)$$

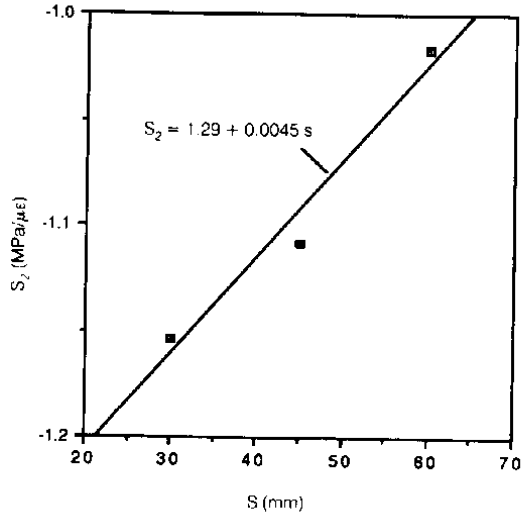


**Fig. 9. Variatioln of the slope $S_2$ with tie spacing.**

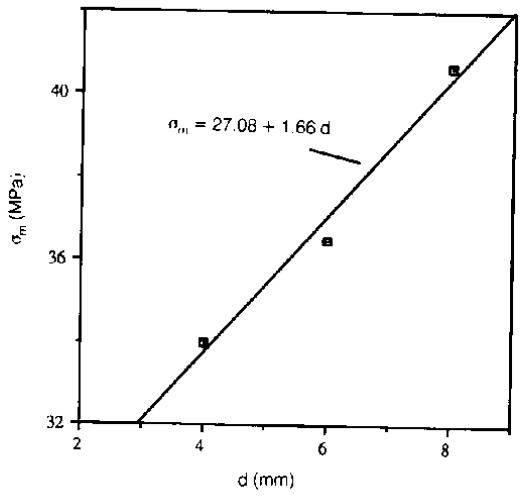


**Fig. 10. Variation of the maximum stress with tie diameter.**

the slope $S_1$ was then expressed as a linear combination of (s) and (d) in the form:

$$S_1 \quad a\,[F(s\,,d)] + b \qquad (MPa/\mu\varepsilon) \qquad (3a)$$

where

$$F(s\,,d) = 0.8\,s - 1.67\,d \qquad (3b)$$

a and b are constants.

Values of F (s, d) were evaluated for the various prisms and plotted against $S_1$ from which a straight line fit resulted in the following equation:

$$S_1 = -46.34 + 0.48\,s - d \qquad (MPa/\mu\varepsilon) \qquad (4)$$

Similarly, the following relations were also obtained:

$$S_2 = -0.97 + 0.005\,s - 0.55\,d \qquad (MPa/\mu\varepsilon) \qquad (5)$$

$$\sigma_m = 36.25 - 0.13\,s + 1.11\,d \qquad (MPa) \qquad (6)$$

$$\varepsilon_m = 3003 - 6.88\,s + 55.52\,d \qquad (\mu\varepsilon) \qquad (7)$$

**Proposed Model**

Having determined the parameters defined by Eqs. (4) to (7), the stress-strain curve may now be obtained by integrating the equations for lines AB and BC, in Fig. 11, in conjunction with these parameters. Consider line AB and let its equation be:

$$E_t \quad \frac{d\sigma}{d\varepsilon} = a_1 + S_1\,\varepsilon \qquad (8)$$

where $a_1$ = constant. Integrating with respect to $\varepsilon$ gives

$$\sigma = a_1\,\varepsilon + 0.5\,S_1\,(\varepsilon^2) + b_1 \qquad (9)$$

where $b_1$ = constant.

Similarly, the equation for line BC would give:

$$E_t = \frac{d\sigma}{d\varepsilon} = a_2 + S_2\,\varepsilon \qquad (10)$$

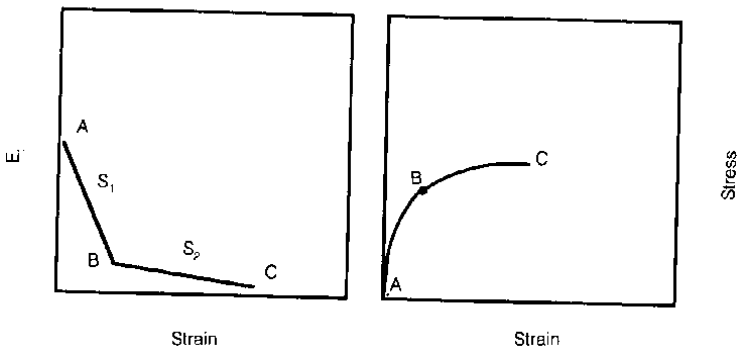


**Fig. 11. Idealization of the $E_t - \varepsilon$ relationship.**

$$\sigma = a_2 \varepsilon + 0.5 S_2 (\varepsilon^2) + b_2 \tag{11}$$

where $a_2$ and $b_2$ are constants. The stress-strain curve is therefore represented by two second-degree parabollae which met at point B as illustrated in Fig. 11. In order to solve Eqs. (9) and (11) with the four unknown constants; four boundary conditions must be satisfied. These conditions are:

1) At point A: $\sigma = 0$ and $\varepsilon = 0$
2) At point B: assuming a common strain ($\varepsilon_B$)
   $(\sigma)_{AB} = (\sigma)_{BC} = \sigma_B$
3) At point C: $\sigma = \sigma_m$ and $\varepsilon = \varepsilon_m$
4) At the same point C: $E_t = 0$

substituting the boundary conditions in equations (8) to (11) produced the following constant values:

$$a_1 = \frac{\sigma_m + 0.5 (\varepsilon_B)^2 (S_2 - S_1) + 0.5 S_2 (\varepsilon_m)^2 - S_2 \varepsilon_m \varepsilon_B}{\varepsilon_B} \tag{12}$$

$$b_1 = 0 \tag{13}$$

$$a_2 = - S_2 \varepsilon_m \tag{14}$$

$$b_2 = \sigma_m + 0.5 S_2 (\varepsilon_m)^2 \tag{15}$$

The evaluation of $a_1$ requires the evaluation of the value of ($\varepsilon_B$). This was determined by equating $E_t$ at the common point B for both curves and using equation (8) and (10) to give the following relationship:

$$\varepsilon_B = \sqrt{\frac{2\,[\sigma_m + 0.5\,S_2\,(\varepsilon_m)^2\,]}{(S_2 - S_1)}} \tag{16}$$

the constant $a_1$ can then be expressed as:

$$a_1 = (S_2 - S_1)\,\varepsilon_B - S_2\,\varepsilon_m \tag{17}$$

The final proposed stress-strain equation is therefore, given as:

$$\sigma = 0.5\,S_1\,(\varepsilon)^2 + [(S_2 - S_1)\,\varepsilon_B - S_2\,\varepsilon_m - S_2\,\varepsilon_m]\,\varepsilon \qquad ;\, 0 \leq \varepsilon \leq \varepsilon_B \tag{18a}$$

$$\sigma = 0.5\,S_2\,(\varepsilon)^2 - S_2\,\varepsilon_m\,\varepsilon + \sigma_m + 0.5\,S_2\,(\varepsilon_m)^2 \qquad ;\, \varepsilon_B \leq \varepsilon \leq \varepsilon_m \tag{18b}$$

where $S_1$, $S_2$, $\sigma_m$ and $\varepsilon_m$ are given by equations (4) to (7), respectively. The analytical ($\sigma - \varepsilon$) curves were then obtained by substituting the values of (d) and (s) for the various prisms and were compared with the experimental curves as shown in Fig. 12. As can be seen from these figures, the proposed model produced a good prediction of the prisms stress-strain behavior for the various tie spacings and diameters.

## Summary and Conclusions

1. An analytical model for describing the ascending branch of the stress-strain curve for concrete prisms confined by rectilinear reinforcement with various spacings and diameters was derived. The concrete prisms were tested in compression under uniaxial uniform load. Based on the observed degradation of the prisms tangent stiffness with respect to the longitudinal strain, a bi-linear idealization of the behavior was assumed. The slopes of the two lines were related to the test variables and a stress-strain relationship consisting of two second degree curves was obtained. When compared with the limited number of tests and investigation variables, the analytical model seems to be very promising.

2. The good accuracy obtained by the derived ($\sigma - \varepsilon$) equation indicated that the ($E_t - \varepsilon$) relationship suitably represents the prism behavior as it reflects the two dominant stages of its stress-strain behavior. The proposed model can also be easily

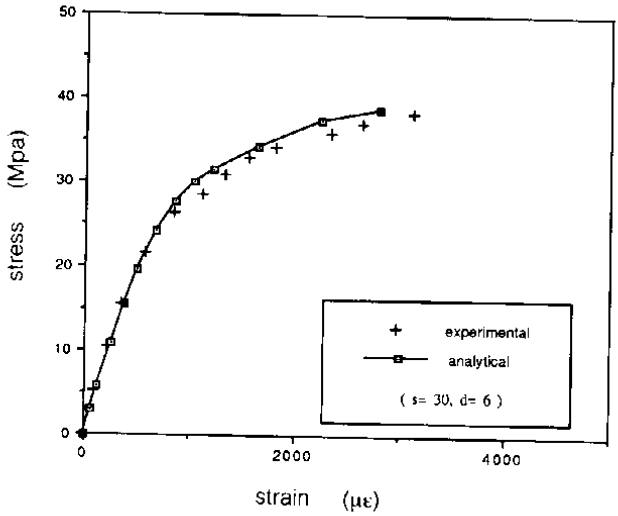


**Fir. 12. Comparison of experimental and analytical stress-strain curves.**

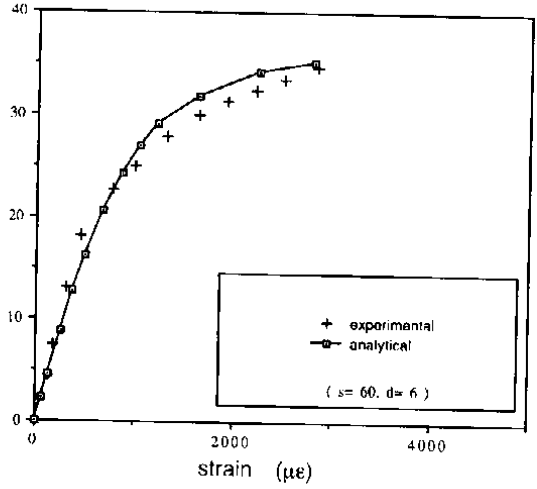


**Fig. 12. (Continued)**

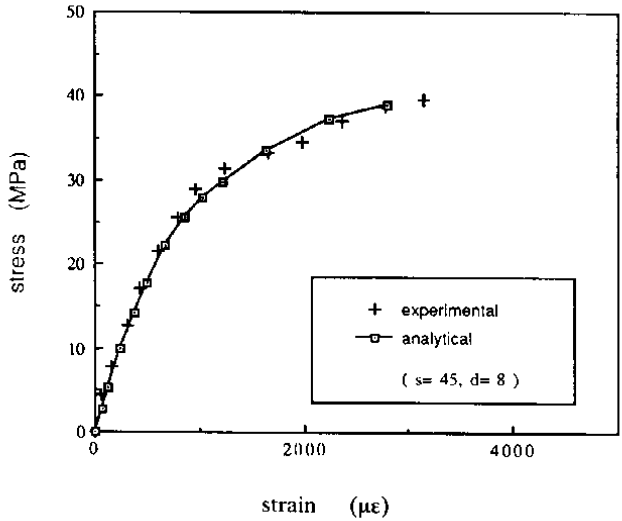


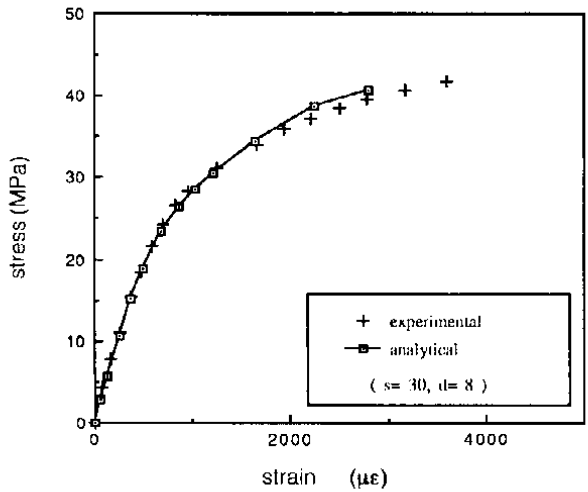


**Fig. 12. (Continued)**

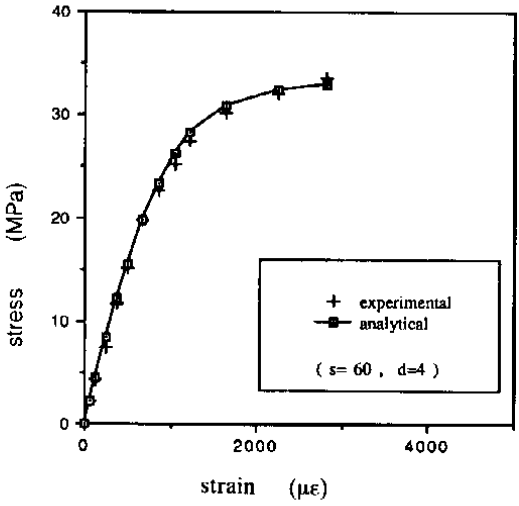


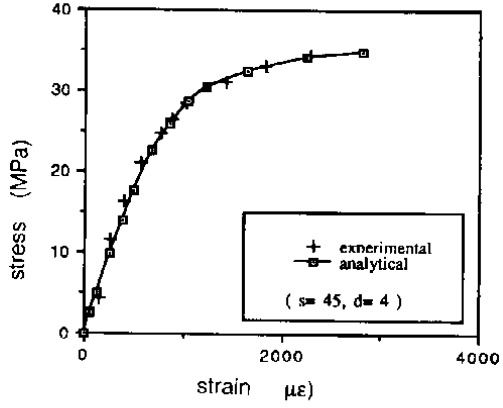


**Fig. 12. (Continued)**

modified by including more test variables, such as concrete strength, and by studying its applicability to spiral or other types of confinement.

## References


[1] Chan, W.W. "The Ultimate Strength and Deformation of Plastic Hinges in Reinforced Concrete Frameworks." *Mag. of Concrete Research*, 2, No. 7 (1955), 121-132.

[2] Roy, H.E. and Sozen, M.A. "Ductility of Concrete." *International Symposium on Flexural Mechanics of Reinforced Concrete*, ACI SP-12, (1964), 213-234.

[3] Soliman, M.T. and Yu, C.W. "The Flexural Stress-strain Relationship of Concrete Confined by Rectangular Transverse Reinforcement." *Mag. of Concrete Research*, 61, No. 19 (1967), 223-238.

[4] Somes, N.F. "Compression Tests on Hooped-reinforced Concrete." *Proc. ASCE, Jour. of St. Div.*, 96, No. ST7 (1970), 1495-1509.

[5] Iyenger, K.T.; Desayi, P. and Reddy, K.N. "Stress-strain Characteristics of Concrete Confined in Steel Binders." *Mag. of Concrete Research*, 72, No. 22 (1970), 173-184.

[6] Sargin, M.; Ghosh, S.K. and Handa, V.K. "Effects of Lateral Reinforcement upon the Strength and Deformation Properties of Concrete." *Mag. of Concrete Research*, 75-76, No. 23 (1971), 99-110.

[7] Sheikh, S.A. and Uzumeri, S.M. "Analytical Model for Concrete Confinement in Tied Columns." *Proc. ASCE, Jour. of ST. Div.*, 108, No. ST12 (1982), 2703-2722.

[8] Ahmed, S.H. and Shah, S.P. "Stress-strain Curves of Concrete Confined by Spiral Reinforcement." *ACI Jour.*, 79, No. 6 (1982), 484-490.

[9] Martinez, S.; Nilson, A.H. and Slate, F.O. "Spirally Reinforced High-strength Concrete Columns." *ACI Jour.*, 81, No. 5 (1984), 431-442.

[10] Dilger, W.H.; Koch, R. and Kowalczyk, R. "Ductility of Plain and Reinforced Concrete under Different Strain Rates." *ACI Jour.*, 81, No. 1 (1984), 73-81.

[11] Sakai, K. and Sheikh, S.A. "What Do We Know About Confinement in Reinforced Concrete Columns ? A critical review of previous work and code provisions." *ACI Structural Jour.*, 86, No. 2 (1989) 192-207.

[12] Cheong, H.K. "Laterally Confined Concrete Prisms under Various Axial Load Conditions." *Ph.D. Thesis*, University of London, (1985).

# العلاقة بين الإجهاد والانفعال في الخرسانة المسلّحة عرضيًّا بطريقة تناقص الصلابة

عبدالرحمن بن حسن آل الشيخ

*قسم الهندسة المدنية، كلية الهندسة، جامعة الملك سعود، ص.ب ٨٠٠، الرياض ١١٤٢١، المملكة العربية السعودية*

(استُلم في ١٦/١١/١٩٩٢م؛ قُبل للنشر في ١٦/٤/١٩٩٣م)

**ملخص البحث.** يتم في هذا البحث استنتاج علاقة بين الإجهاد والانفعال الناتج عنه في الخرسانة المسلحة عرضيًا بكانات حديدية والواقعة تحت أحمال ضغط منتظمة التوزيع، باستخدام نتائج دراسة تجريبية أجريت على نماذج مصغرة لأعمدة خرسانية. فبدراسة طريقة تناقص معامل الصلابة المماسي للأعمدة مع الانفعال أمكن افتراض علاقتين خطيتين بينهما وربطهما بمتغيّرات الاختبار والاجهاد الكلي والانفعال المصاحب له، ومن ثم استخدامها في استنتاج العلاقة بين الإجهاد والانفعال. وقد تم التحقق من دقة العلاقة المستنتجة بمقارنتها بنتائج تجريبية.